Sensors & Transducers, Vol. 203, Issue 8, August 2016, pp. 51-56

Sensors & Transducers

Measuring Millimeter Wave of Cold Atmospheric Plasma Array by a Novel Technique

[1] Bryon Eckert, [1] Bradley Eckert, [1] Huan Truong and [2] Mina Izadjoo
[1] Trideum Biosciences, Frederick, MD, USA
[2] Chiscan LLC, Tempe, AZ, USA
E-mail: mizadjoo@trideumbiosciences.com, bryon@chiscan.com

Received: 9 July 2016 /Accepted: 29 July 2016 /Published: 31 August 2016

Abstract: An unexplained repulsive force occasionally observed during non-thermal plasma treatment of large infections may point the way to an efficient mechanism for characterizing biofield energy. Ambient pressure air plasma in non-thermal equilibrium creates areas of localized population inversion, causing spontaneous emission at magnetic dipole rotational resonance lines. For O_2, many of these lines occur in the 60 GHz frequency range. This experiment examines a possible link between the fine resonance frequencies of oxygen in the 60 GHz region, and the therapeutic frequencies used in Russian non-thermal EHF therapy. This paper also explores the feasibility of using a plasma array for biological torsion field characterization. An array of several hundred non-thermal plasma plumes are placed directly in front of a circular horn. A switchable circular polarizer is used to select left hand circular, linear or right hand circular polarization. A low noise frequency converter allows a noise temperature of less than 1150 K. A frequency scan and averaging algorithm is developed to characterize noise temperature versus frequency, comparing signal and noise levels between plasma on and plasma off, and switching polarization sense. An experimental setup is proposed as a proof of concept for detecting signals from the plasma array, while a practical laboratory tool is also proposed. *Copyright © 2016 IFSA Publishing, S. L.*

Keywords: EHF, biological, plasma, polarization

1. Introduction

Numerous published papers have noted biological effects based on the modulation frequency of non-thermal air plasma [1]. Another energetic biological effect which has been widely studied in Eastern Europe is non-thermal EHF radiation. Some common therapeutic frequencies are 53.6 GHz and 61.2 GHz [2], corresponding to some of the fine resonance frequencies of oxygen in the 60 GHz [3].

Power levels range from 1 pW/cm^2 to 10 mW/cm^2, and biological effects are weakly related to power level. A typical signal source for EHF therapy is a cavity stabilized Gunn or IMPATT oscillator, frequency modulated over a 10 MHz bandwidth to ensure the source frequency sweeps over the precise oxygen fine resonance. Alternatively, the signal source may be an IMPATT device which generates broadband noise between 40 and 80 GHz at the microwatt level.

Since frequency selective EHF therapeutic effects have been observed at extremely low power levels, a search for 60 GHz energy from an array of non-thermal air plasma plumes may provide additional data for examining the therapeutic mechanisms of plasma medicine.

A typical plasma array element is shown in Fig. 1. The top element is a metal ring with protruding points to concentrate the electric field, initiating plasma discharge in defined areas. The substrate material is 200um thick FR4, and the plasma is driven at about 100 kHz. Within the area of the horn opening are about 50 plasma elements or 300 plasma plumes.

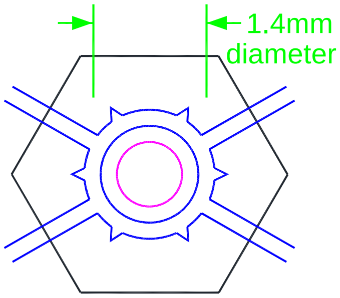

Fig. 1. Plasma array element.

The electrical distance between plasma points along the microstrip ring is about λ/4 at 60 GHz. During each cycle of the driving waveform, the initiation of plasma discharge creates a localized non-homogeneous magnetic field pulse. This separates out atoms with higher energy state, and hence creates localized areas of population inversion.

The resonant mutual coupling between the elements in the plasma array should create a mechanism for spontaneous and possibly stimulated emission at the various fine resonance frequencies of oxygen in the 60 GHz range.

Because the effect would most likely occur in the nanosecond region, it would be seen as radio carriers combined with broadband noise side-bands. The carriers could be efficiently characterized with a large FFT.

The carriers we expect to see will be modified by Zeeman splitting, from the earth's magnetic field. Interaction between any time varying components of the biofield and the plasma will generate additional carriers.

The biofield is purported to consist of torsion waves, in which time and gravitation serve as counterparts to the electric and magnetic components of a transverse electromagnetic wave. However, the torsion wave is scalar, hence the torsional component. Electromagnetism is illustrated in Fig. 2, and a torsion wave in Fig. 3.

A slight non-linearity in the medium can result in a small static electric or magnetic component, which has been detected by numerous methods. If we assume that the biofield carries information as a dynamic component, then a vast amount of information remains undetected.

Since the torsion wave does not have a transverse component, it cannot be detected by an antenna. It can be detected by an electron avalanche such as that contained within the plasma, since a variation in time rate density will influence electron momentum. Electron spin polarization may also detect torsion waves [4].

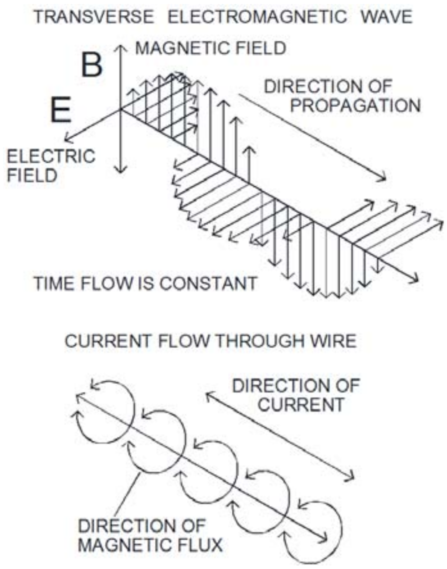

Fig. 2. Electromagnetic interactions.

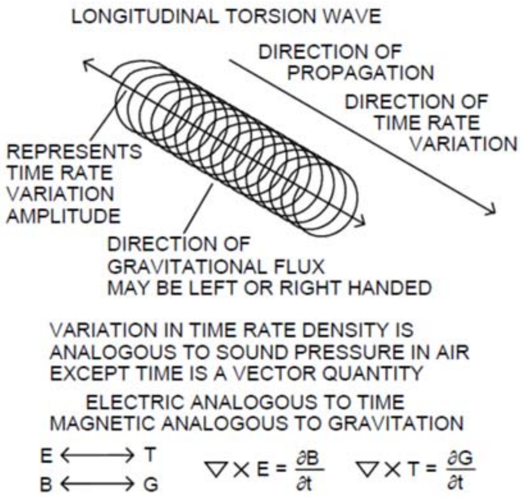

Fig. 3. Torsion wave hypothesis.

It is possible that biofield torsion wave spin may impart a circular polarization to some radiated carriers. Also, circular polarization is commonly observed in astrophysical masers, so this may occur with the plasma array through Zeeman interaction with the associated magnetic fields. In EHF therapy, biological effects have been linked with circular polarization, with effects observed only with the correct polarization [5].

The atmospheric absorption of oxygen has created commercial interest in 60 GHz short range radio development. A 60 GHz receiver module can be used in a relatively inexpensive apparatus designed to search for low level microwave signals from a plasma array.

For a practical instrument, however, the entire RF bandwidth should be analyzed at the same time. This can be accomplished with a high gain low noise amplifier followed by a harmonic mixer.

2. Proof of Concept

A block diagram of the experiment setup is shown in Fig. 4. The circular horn, switchable circular polarizer and associated circular to linear waveguide transition are purchased from Quinstar.

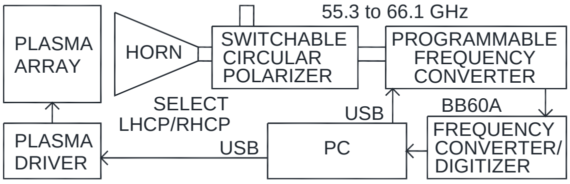

Fig. 4. Experiment Block Diagram.

The heart of the programmable frequency converter is a 60 GHz SiGe receiver module currently distributed through Pasternack Enterprises. The receiver module has the following features:

- WR-15 waveguide input with standard flange;
- Noise Figure: 6.0 dB typical;
- Gain: 38 dB minimum at 1.65 GHz IF;
- Power dissipation: 600mW typical.

A block diagram of the receiver module is shown in Fig. 5. The low side image from the sliding IF, which is around 45 GHz at a maximum, is filtered by the LNA design. The synthesizer frequency dividers are determined by the allowable programmable divider output frequency.

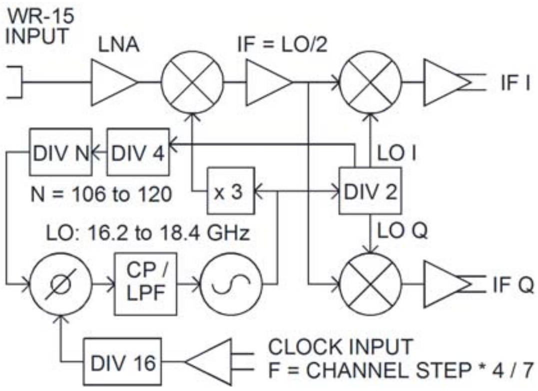

Fig. 5. 60 GHz Receiver Module Block Diagram.

The programmable frequency converter block diagram is shown in Fig. 6. A 2.4 GHz frequency synthesizer and associated frequency divider generate the reference clock for the synthesizer inside the receiver module.

A quadrature coupler and associated switches are used to select between upper and lower IF sideband, extending the usable frequency coverage of the receiver within the bandwidth limits of the LNA.

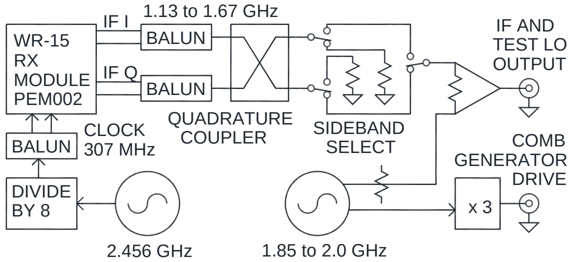

Fig. 6. Frequency Converter Block Diagram.

A separate frequency synthesizer generates a signal for testing the converter. This can be used to test proper synthesizer programming, opposite sideband rejection, and antenna axial ratio. The basic frequency range is 1.85 to 2.0 GHz. This is routed through a signal combiner to the IF output for verifying the test synthesizer.

The test synthesizer frequency is also multiplied by 3 by a chain of multiplier, filters and amplifiers. Typical output level is +13 dBm, suitable for driving an external Schottky diode as a comb generator for generating test signals in the 60 GHz range. A photo of the programmable frequency converter is shown in Fig. 7.

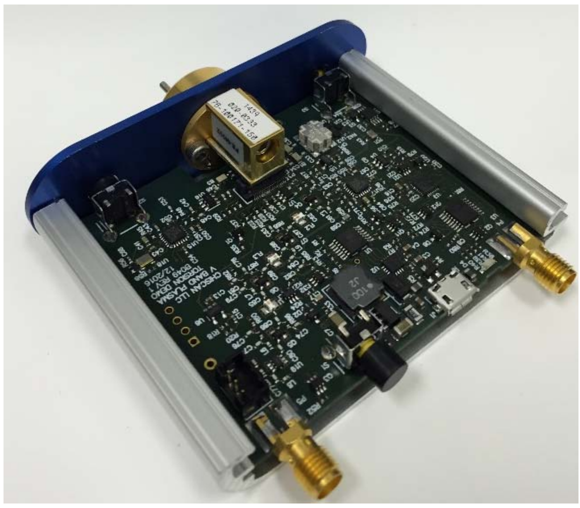

Fig. 7. 60 GHz Programmable Frequency Converter.

The IF output from the programmable frequency converter connects to a Signal Hound BB60A spectrum analyzer. This is actually a tunable frequency converter and digitizer, since the spectral analysis is performed on an external PC.

The BB60A ADC sample rate is 80 MSPS, and the usable analysis bandwidth of 20 MHz is set by the SAW filters before the ADC. A block diagram of the BB60A as used in the specified range of 1.13 to 2.0 GHz is shown in Fig. 8.

The data from the ADC is routed through an FPGA and Cypress FX3 USB3.0 bridge to a PC. Because of the high continuous data rate, the

CPU should be at minimum Intel i7 third generation quad core.

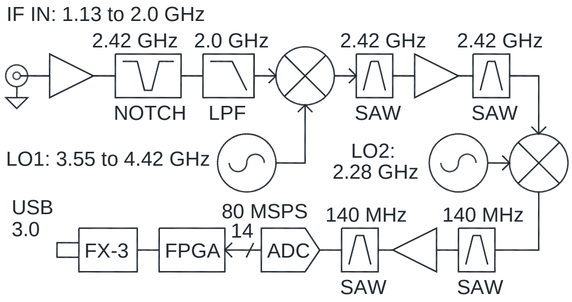

Fig. 8. BB60A Block Diagram.

Spectral analysis is done by FFT to improve analysis speed. For the 80 MSPS sample rate, an FFT size of N=2^16 creates an equivalent noise bandwidth of 1.8 kHz and requires a plasma on time of about 1ms.

The frequency reference for the synthesizers inside the 60 GHz programmable frequency converter is a 40 MHz TCXO. The synthesizers are Analog Devices ADF4360 series integer N with internal VCO. To minimize the phase noise floor, a high frequency is used on the phase detector.

The step size of the receiver module synthesizer is 7/4 of the clock. A clock frequency of 307 MHz minimizes the clock synthesizer noise floor, and sets the receiver synthesizer step size to 537.25 MHz. The I and Q IF outputs are connected to a quadrature hybrid coupler. The coupler outputs are switched to pass either the high side or low side IF frequency, and reject the opposite sideband.

Although the synthesizer covers 15 channels, some channels are set to low side IF output. Setting the sideband sense along with the LO channel frequency makes a total of 21 receiver channels between 55.28 and 66.14 GHz.

The BB60A spectrum analyzer acts as a programmable frequency converter. Since the first IF frequency is 2420 MHz with 20 MHz bandwidth, the first synthesizer is programmed to tune from 3560 to 4080 MHz in 20 MHz steps.

Each IF scan uses a total of 27 channels, except for the frequency overlap when the IF sideband is switched from low to high. In this case, 21 channels can be skipped. For a full frequency scan, a measurement is performed on a total of 546 IF channels. If the plasma is run at 50 % duty cycle, a full frequency scan can be completed in about 1 second.

3. Practical Analysis Tool

The proof of concept receiver can be improved by widening the frequency coverage to cover the entire oxygen resonance band of 53 to 67 GHz. This can be done by building a custom microwave module with electronic polarization switching, a high gain low noise amplifier, and harmonic mixer. A block diagram of this module along with supporting electronics is shown in Fig. 9.

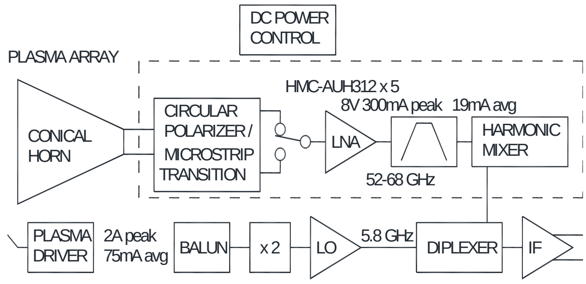

Fig. 9. Plasma based sensor module.

The intended size of the sensor box is 2×2×4 inches. The local oscillator operates at 5.8 GHz to support a future semiconductor based pulsed avalanche sensor, which will reduce cost and size. The IF is designed to operate to 2.9 GHz.

The wide IF bandwidth is digitized in a 7.7 ms burst. This retains the phase relationships between all carriers at the complex FFT output. The FFT size is designed to support a practical DRAM bandwidth and power consumption for a future ASIC design.

The ADC sampling rate is set at 1.5 times the receiver sampling rate. This aliases the 5.8 GHz receiver local oscillator down to 2.9 GHz at the FFT output while allowing the IF to go up to 2.9 GHz. The FFT size of 2^26 samples is likely to be processed in 210ms in the future ASIC design.

Running the plasma for 10 ms every 220 ms reduces ozone production and plasma driver power dissipation by reducing the plasma duty cycle to 4.5 %. The low duty cycle also reduces power dissipation in the digitizer electronics.

A digitizer is constructed using commercially available high speed ADCs where the data is captured in a burst to DRAM, then sent to a PC at a slower rate over an SPF+ optical transmitter. A block diagram of the converter is shown in Fig. 10.

An external frequency reference will be used, preferably very stable such as a GPS disciplined rubidium stabilized source. The high speed FFT is done in the PC, using a GPU card for reduced power consumption. The digitizer and sensor cost will be relatively high but can be reduced in the future with an ASIC design.

4. Solid State Sensor

We envision the use of a plasma array as a biofield sensor as just a stepping stone to a technology that can be more broadly used. The plasma array has the advantage of relatively low development cost, but high unit cost.

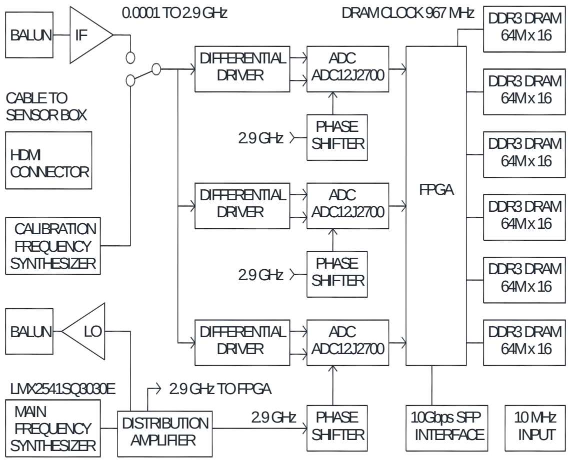

Fig. 10. Digitizer block diagram.

Spin-spin interaction has been observed with circular polarized laser beams in a vapor chamber, and with spin polarized protons, so it is likely that high frequency torsion energy will interact with spin polarized electrons.

Our proposed device has the following features:

- Production of net electron spin polarization using circularly polarized light;
- Long range interaction between torsion wave and electron spin polarization;
- Electronic detection of interaction through spin dependent trap assisted tunneling;
- Electronic signal amplification through an avalanche mechanism;
- Sub-harmonic frequency mixing by modulating the avalanche bias voltage.

For the active area of our device, we fabricate a 4H-SiC membrane using molecular beam epitaxy. The top and bottom electrodes have holes to allow light to pass through, inducing electron spin with circularly polarized light. The top electrode is a schottky contact to lightly doped SiC, and the bottom electrode is an ohmic contact created by a thin heavily doped SiC layer. The proposed device is shown in Fig. 11.

To minimize electric field crowding at the edges of the holes, we subject the exposed top SiC to an argon ion implant. This also creates lattice defects that cause reverse current leakage through an electron tunneling mechanism. The device is biased close to breakdown, so the reverse leakage current initiates an electron avalanche within the SiC membrane.

The proposed device will have the advantage of small size and low cost. Since the avalanche bias will be driven by an AC signal at a relatively high voltage (in addition to a DC bias), the module will tend to radiate at a high enough level that radio regulations will need to be considered. For this reason, the international 5.8 GHz ISM band is used.

The proposed device thickness will have a propagation delay of about 8 ps, so the avalanche process will produce an IMPATT mechanism in the 60 GHz range. Adding a suitable amount of on-chip inductance will resonate the electrode capacitance and produce “ringing” in the 60 GHz range.

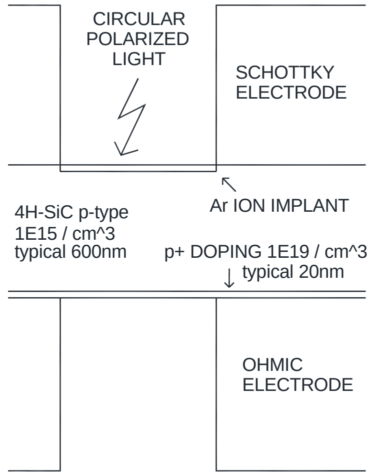

Fig. 11. Silicon Carbide Avalanche Device.

This ringing will increase the frequency conversion efficiency at 60 GHz and harmonics. If we assume the frequency content of the biofield to be related to the rotational resonances of oxygen, the frequency stability of the system should be designed to allow detection to 2.5 THz.

Initially, this sensor would be used with the digitizer proposed in Fig. 10, and the associated PC. However, the digitizer and PC can eventually be replaced with an ASIC, most likely fabricated in a 16 nm FinFET process.

Because of the large FFT size, cost is minimized by using off-chip DRAM. DRAM bandwidth will require some care to minimize power consumption. A suitable interface is the Kandou Glasswing bus, clocked at 11.6 GHz. A common strategy is to do a 2D FFT (at 2^13 in our case), storing intermediate results. A total of three 8Gb memory die would be used inside the ASIC package.

Some sections of this article was included in a poster presentation in the 2016 TechConnect World Innovation Conference held in May 23-25, 2016. National Harbor, Maryland, USA [6].

References

[1]. M Alkawareek, Q Algwari, G Laverty *et al*, Eradication of Pseudomonas aeruginosa Biofilms by Atmospheric Pressure Non-thermal Plasma, *PLoS One*, 7, 8, 2012, p. e44289.

[2]. M. Logani, M. Bhopale and M. Ziskin, Millimeter Wave and Drug Induced Modulation of the Immune System - Application in Cancer Immunotherapy, *J. of Cell Science and Therapy*, S5, 2011.

[3]. J. Burkhalter, R. Anderson, W. Smith, W Gordy, The Fine Structure of the Microwave Absorption Spectrum of Oxygen, *Physical Review*, Vol 79, 1950, pp. 651-655.

[4]. R. Hammond, Spin Flip Probability of Electron due to Torsional Wave, *Physical Review D,* Vol. 90, September 2014, p. 067501.
[5]. I. Belyaev, Non-thermal Biological Effects of Microwaves, *Mikrotalasna revija / Microwave Review,* November 2005, pp. 13-29.
[6]. B. Eckert, B. Eckert, H. Truong and M. Izadjoo, A Novel Technique of Measuring Millimeter Wave Cold Atmospheric Plasma Array, in *Proceedings of the 2016 TechConnect World Innovation Conference*, National Harbor, Maryland, USA May 23-25, 2016.